Electronic Supplementary Information for

Catalytic CO oxidation over $Pd_{70}Au_{30}(111)$ alloy surfaces: spectroscopic evidence for Pd ensemble dependent activity

Ryo Toyoshima,[a] Nana Hiramatsu,[a] Masaaki Yoshida,[a] Kenta Amemiya,[b] Kazuhiko Mase,[b] Bongjin Simon Mun[c] and Hiroshi Kondoh*[,a]

Author address

[a] Department of Chemistry, Keio University, 3-14-1 Hiyoshi, Kohoku-ku, Yokohama, Kanagawa 223-8522, Japan

[b] Institute of Materials Structure Science, High Energy Accelerator Research Organization, and The Graduate University for Advanced Studies, 1-1 Oho, Tsukuba, Ibaraki 305-0801, Japan

[c] Department of Physics and Photon Science, Gwangju Institute of Science and Technology, Gwangju 500-712, Republic of Korea

*To whom correspondence should be addressed.

E-mail: kondoh@chem.keio.ac.jp

Index **Page**

1. Temperature dependence of CO adsorption on the $Pd_{70}Au_{30}$(111) surface

The temperature dependence of adsorbed CO is important to understand the adsorption behavior of CO. Fig. S1 shows C 1s XP spectra taken from a $Pd_{70}Au_{30}$(111) surface under 10 mTorr CO at different temperatures from 25 to 175 ºC. The comparison indicates that the heating causes partial desorption of CO at top site and a slight increase of CO at bridge/hollow sites. The increase of CO at bridge/hollow sites is associated with a site change from top to bridge/hollow site due to the increase of surface temperature. Note that the atomic carbon probably comes from bulk and a major part of atomic carbon disappears from the surface by the coexistence of O_2 (i.e. under reaction conditions).

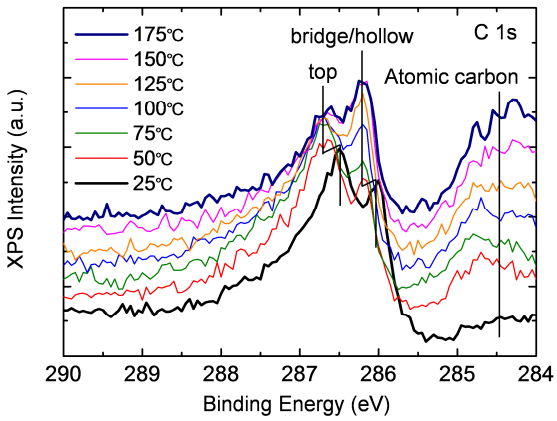

Fig. S1 C 1s XP spectra taken from $Pd_{70}Au_{30}$(111) surfaces under the 10 mTorr CO at different temperatures from 25 to 175 ºC. Coexistence of atomic carbon gives an effect on the binding energies of CO to shift slightly toward the higher energy side.

2. CO adsorption and CO oxidation on the $Pd_{70}Au_{30}$(111) surface at 150 ºC

The increase of temperature causes CO desorption from the surface, and it ignites the catalytic reaction. The CO desorption is in equilibrium with adsorption from the gaseous CO in the present experimental condition. The CO coverage on the surface gradually decreases with increasing temperature as shown in Fig. 2b. The decrease and disappearance of the CO at top site could be contributed at least partially from the thermal desorption. Fig. S2 shows the C 1s XP spectra taken under 10 mTorr CO ambient and that under a reaction condition (P_{O2} = 100 mTorr and P_{CO} = 10 mTorr) at 150 ºC. At this temperature, the catalytic reaction already proceeds as shown in Fig. 2b. If the CO at top site is the catalytically active species, the peak intensity of CO at top site should be decreased by the reaction with oxygen atoms. In fact, the fractional ratio of CO at top site, I_{top} / (I_{top} + $I_{bridge/hollow}$), is decreased from 0.54 under 10 mTorr CO to 0.49 under the reaction condition, i.e. P_{O2} = 100 mTorr and P_{CO} = 10 mTorr. It indicates that the CO at top site is more rapidly consumed under the reaction condition compared to the CO at bridge/hollow sites. Note that the decrease in the coverage of CO at top site by introducing additional O_2 gas (100 mTorr) was checked using the fractional ratio, because the XPS peak intensity cannot be directly compared unless the total pressure keeps constant.

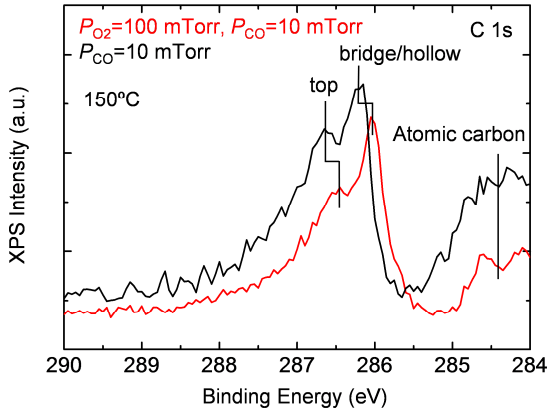

Fig. S2 C 1s XP spectra taken from $Pd_{70}Au_{30}$(111) surfaces under exposing to 10 mTorr CO at 150 ºC (black) and under a reaction condition (P_{O2} = 100 mTorr and P_{CO} = 10 mTorr) at 150 ºC (red). Coexistence of atomic carbon gives an effect on the binding energies of CO to shift slightly toward the higher energy side.

3. Adsorption energies of CO and oxygen on the Pd(111) and Pd−Au(111) surfaces

For density functional theory (DFT) calculations, Vienna ab initio simulation package (VASP) was employed to investigate the adsorbate−metal interactions on the Pd(111) and Pd−Au(111) surfaces. The projector-augmented wave (PAW) method and the Perdew−Burke−Ernzerhof (PBE) approximation were applied to represent the electron−ion and exchange−correlation interactions, respectively. For the bulk calculations, the Pd and $Pd_{75}Au_{25}$ bulk crystals were modeled by *A*1 (fcc) and $L1_2$ structures, and resultant equilibrium lattice constants were 3.95 and 4.01 Å, respectively. The surface calculations were performed by the slab and supercell approaches. The metal surfaces were modeled by a four-layer slab with a vacuum space (> 10 Å), where the upper two substrate layers and adsorbates were relaxed until the residual force was < 0.05 eV/Å for each atom. The (4 × 4) supercell was integrated with (3 × 3) *k*-point mesh with the Monkhorst−Pack method.

Table S1 shows the calculated adsorption energies of CO and atomic oxygen on Pd(111) and Pd−Au(111) surfaces. The adsorption energy is estimated by the difference in the total energies of adsorbate−metal, bare metal and isolated free molecule systems. CO prefers the mono-elemental sites, while the adsorption of CO on a bi-elemental site is less stable, for example the top site on Pd_1 provides the higher adsorption energy than the bridge site on Pd_1Au_1 ensemble. The oxygen adsorption is realized exclusively at hollow sites on both mono- and bi-elemental ensembles.

Table S1 Calculated adsorption energies (E_{ad}) of CO and oxygen (O) on Pd(111) and Pd−Au(111) surfaces, which are obtained with respect to isolated free molecules. Here, the regular adsorption sites on (111) surface; hollow (H), bridge (B) and top (T) are tested for each adsorbate.

system	site	E_{ad} (eV)
CO/Pd−Au(111)	H(Pd_3)	−1.87
	B(Pd_2)	−1.50
	T(Pd_1)	−1.15
O/Pd−Au(111)	H(Pd_3)	−0.91
	H(Pd_2Au_1)	−0.58
	H(Pd_1Au_2)	−0.10
CO/Pd(111)	H(Pd_3)	−1.93
	B(Pd_2)	−1.77
	T(Pd_1)	−1.34
O/Pd(111)	H(Pd_3)	−1.31

4. XPS results for in-plane Pd aggregation

As discussed in the previous work[1], CO adsorbs at surface-segregated Pd sites. Moreover, the local Pd configurations link to the adsorption site; the Pd monomer, dimer and trimer reflect the top, bridge and hollow sites, respectively. Here the surface Pd distribution before and after the O_2 exposure is probed by adsorbed CO as shown in Fig. S3. C 1s XP spectra taken under a reaction condition (P_{O2} = 100 mTorr and P_{CO} = 10 mTorr) at 30 ºC are compared between surfaces after cleaning (fresh) and 100 mTorr O_2 exposure at 300 ºC. The CO adsorption leads two distinct peaks at 286.1 and 286.6 eV, assigned to CO at bridge/hollow sites and top sites, respectively. A small feature at around ~285 eV is carbon residuals, while a peak at ~291 eV is assigned to the gaseous CO. It is noted that the difference in gaseous peak intensity comes from a slight variation of the sample−aperture distance. It is obvious that the intensity ratios of CO are different between bridge/hollow and top sites, indicating that the amount of contiguous Pd ensemble, which provides bridge/hollow sites, is increased by the O_2 exposure.

Table S2 shows Pd/Au elemental ratios under given conditions. The ratio is estimated to be 0.51 at the (well-annealed) clean surface. The Pd $3d_{5/2}$ and Au $4f_{7/2}$ levels were measured with almost the same photoelectron kinetic energies. It is noted that the photoionization cross-section is not taken into accounts, thus this value does not indicate the absolute Pd/Au elemental ratio. This value is essentially unchanged by the O_2 exposure (P_{O2} = 100 mTorr) and the reaction condition (P_{O2} = 100 mTorr and P_{CO} = 10 mTorr), which indicates that the surface segregation of Pd from bulk does not occur in the present experimental conditions.

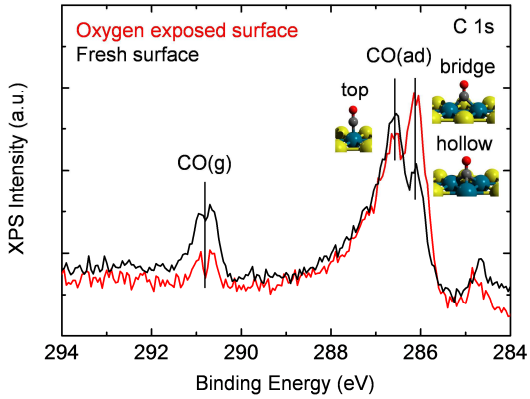

Fig. S3 C 1s XP spectra taken from $Pd_{70}Au_{30}$(111) surfaces under exposure of a gas mixture (P_{O2} = 100 mTorr and P_{CO} = 10 mTorr) at 30 ºC. The surfaces are obtained by a standard cleaning procedure (fresh) and after the 100 mTorr O_2 exposure at 300 ºC.

Table S2 Comparison of Pd/Au elemental ratio deduced from Pd $3d_{5/2}$ and Au $4f_{7/2}$ peak intensities (I). Here, the Pd $3d_{5/2}$ and Au $4f_{7/2}$ levels are recorded by the photon energies of 430 and 180 eV, respectively.

condition	$I_{Pd\ 3d}/(I_{Pd\ 3d}+I_{Au\ 4f})$
clean at 30 ºC	0.52
O_2 exposure at 250 ºC	0.51
CO oxidation at 250 ºC	0.51

5. Oxygen adsorption on the $Pd_{70}Au_{30}(111)$ surface under 100 mTorr O_2 ambient

To understand the oxygen adsorption on $Pd_{70}Au_{30}(111)$ surfaces is important to investigate the catalytic CO oxidation. Fig. S4 shows the O 1s and Pd $3d_{5/2}$ XP spectra taken from a $Pd_{70}Au_{30}(111)$ surface under 100 mTorr O_2 ambient at 300 ºC. The O 1s level exhibits a peak at 529.3 eV associated with chemisorbed oxygen. The estimated oxygen coverage is 0.15 monolayer (ML), which is less than that on Pd(111) (0.25 ML). It is noted that the oxygen adsorption was not observed at a low temperature (30 ºC). The surface oxide formation is observed on Pd(111) surface under similar pressure and temperature conditions, which gives doublet peaks corresponding to the surface and interface oxygen species in O 1s level.[2] Whereas the present O 1s level shows a single peak. This leads us to attribute this peak to a chemisorbed state on $Pd_{70}Au_{30}(111)$ surface, though the oxide formation is not completely excluded. The Pd $3d_{5/2}$ level exhibits two oxygen-induced components. For the accurate peak assignment, the experimental core-level shifts (CLSs) are compared with the calculated results based on the Slater−Janak transition state approximation.[3] The calculated and experimental CLSs are summarized in Table S3. Here, two types of oxygen-induced CLS are found on the surface, which are different in the oxygen coordination number.

Since oxygen-free surface Pd atoms are observed at 334.6 eV, only a part of surface Pd atoms bind with oxygen. Although hollow sites of Pd_1Au_2, Pd_2Au_1 and Pd_3 ensembles are available for oxygen adsorption, the adsorption energies for these sites are rather low as shown in Table S1. The low adsorption energies may cause the low occupation of the hollow sites. Since the Pd atoms are highly dispersed on the Pd−Au surface, the oxide formation needs a significantly high activation energy than that of Pd(111) due to necessity of a large mass transfer. This is a reason why the contribution of oxide formation is quite limited.

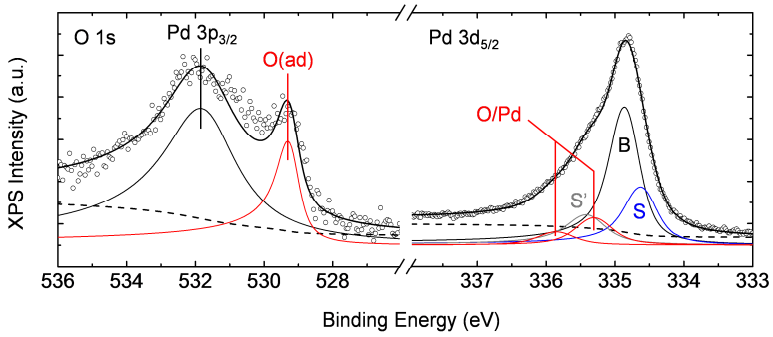

Fig. S4 O 1s and Pd $3d_{5/2}$ XP spectra taken from a $Pd_{70}Au_{30}(111)$ surface under 100 mTorr O_2 ambient at 300 ºC.

Table S3 A comparison of calculated and experimental CLSs. The oxygen (O) atoms are located at hollow sites. The CLSs of Pd $3d_{5/2}$ level are shown with respect to the bulk Pd atom. The oxygen-induced CLSs of Pd $3d_{5/2}$ level are labelled as Pdx, where x means the coordination number of oxygen to a Pd atom.

system	label	calcd CLS (eV)	exp. CLS (eV)
$Pd_{75}Au_{25}(111)$	S	−0.13	−0.26
$O/Pd_{75}Au_{25}(111)$	$Pd_{1/3}$	+0.56	+0.46
	$Pd_{2/3}$	+0.87	+1.00

6. Details of experimental and analysis methods

[Experimental setups]

XPS experiments were performed at the soft X-ray beamline 13B at the Photon-Factory of High Energy Accelerator Research Organization (KEK-PF) in Tsukuba, Japan.[4] AP-XPS measurements were performed by a homemade vacuum chamber.[2] The base pressures of the analysis chamber and the separated preparation chamber were of the order of 10^{-10} Torr. The Pd(111) and $Pd_{70}Au_{30}$(111) surfaces were cleaned by several cycles of Ar^+ sputtering, O_2 treatment and brief annealing up to 750 ºC. The reactant gases (O_2 and CO) were introduced into the analysis chamber via variable leak valves. Incident photon energies were tuned to enhance the surface sensitivity (i.e. O 1s, 630 eV; Pd 3d, 430 eV; C 1s, 380 eV).

[Turn over frequency]

In Fig. 2, the CO coverage is estimated from the peak intensities of adsorbed CO in C 1s level, where the C 1s intensity taken from the CO-saturated Pd(111) surface is used as the standard (0.5 monolayer).[5] Besides, the catalytic CO conversion (C) is estimated from the peak intensities (I) of gaseous CO and CO_2 in C 1s level, $C = I_{CO2} / (I_{CO} + I_{CO2})$. The turn over frequency (TOF) of CO_2 is estimated under the catalytically active condition. Here, it is assumed that the gaseous species is under a molecular flow condition, and all the CO molecules once impinge onto the surfaces and are evacuated via the aperture. It is assumed that the CO molecules impinged to the surface spills over to the Pd site, where the density of reaction site (surface Pd) is 1.0×10^{15} and 3.2×10^{14} cm^{-2} on Pd(111) and $Pd_{70}Au_{30}$(111), respectively. The collision frequency of CO onto a Pd site (z $site^{-1}s^{-1}$) at a CO pressure of 10 mTorr was estimated using the Hertz−Knudsen equation, $p / (2\pi m k_B T)^{1/2}$, to be 3.8×10^3 and 1.2×10^4 $site^{-1}s^{-1}$ on Pd(111) and $Pd_{70}Au_{30}$(111), respectively. At 150 ºC, 14.3 and 9.4% of the introduced CO gas is converted to CO_2. Then the TOF is estimated to be 5.4×10^2 and 1.1×10^3 $site^{-1}s^{-1}$ on Pd(111) and $Pd_{70}Au_{30}$(111), respectively. Although the conversion and slope of conversion are higher in Pd(111) than in $Pd_{70}Au_{30}$(111), the TOF becomes higher in the Pd−Au alloy due to a smaller number of Pd sites.

[Curve fitting analyses]

XP spectra were calibrated with respect to the Fermi edge, and normalized by the base line level, and curve fitted by the convolution of Doniach−Šunjić and Gaussian functions with the Shirley-type background. As an example, results of curve fitting analyses for C 1s XP spectra (Fig. 2a) are shown in Fig. S5.

Fig. 2 shows CO molecules at bridge and hollow sites give close binding energies in C 1s level. However by curve fitting analyses, they can be deconvoluted into distinct components as shown in Fig. S5. Under the reaction condition (P_{O2} = 100 mTorr and P_{CO} = 10 mTorr) at 30 ºC (bottom), we observed three components assigned as CO at hollow site (285.7 eV), CO at bridge site (286.1 eV) and CO at top site (286.6 eV) on the surface and the surface is mostly covered by COs at the bridge and top sites. On the other hand at 300 ºC (top), the peak shifts to the lower binding energy side appearing at 285.7 eV, which indicates that the CO at hollow site is dominantly observed under the active condition.

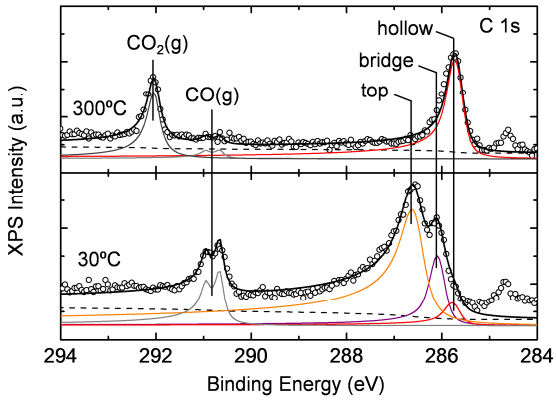

Fig. S5 C 1s XP spectra taken from a $Pd_{70}Au_{30}(111)$ surface under the reaction condition (P_{O2} = 100 mTorr and P_{CO} = 10 mTorr). The XP spectra are the same with ones that shown in Fig. 2a, and curve-fitted into distinct components.

[Peak assignments for the XP spectra]

The Pd $3d_{5/2}$ XP spectrum taken from the $Pd_{70}Au_{30}(111)$ under the reaction condition at 300 ºC (Fig. 3, right panel) shows two additional components (335.2 and 335.7eV), in addition to three components from bulk (B), surface (S) and subsurface (S') which are observed for the clean surface (Fig. 1a). The C 1s XP spectrum shows a peak centered at 285.7 eV indicating that the CO at hollow site is a dominant species (Fig. 2a, top panel), whereas the O 1s XP spectrum shows no signal originating from oxygen species (Fig. 3, left panel). Therefore the both two additional Pd $3d_{5/2}$ components are ascribed to CO-adsorbed species. We reported the peak assignments for Pd $3d_{5/2}$ XP spectra under a high-pressure CO in our previous work.[1] According to the assignments, these components are attributed to Pd bonding with CO at hollow site (335.2 eV) and that at bridge site (335.7eV). From the curve-fitting analyses, it is confirmed that the fraction of CO adsorbed at bridge site is considerably smaller than that at hollow site. In the case of Pd(111), the CO and oxygen adsorption behavior has been extensively investigated. The Pd $3d_{5/2}$ XP spectrum (Fig. 3, right panel) exhibits a single additional component, excepting for two components from bulk (B) and surface (S). The corresponding C 1s XP spectrum shows no peak except for the CO_2 peak (Fig. 2a, bottom panel), whereas the O 1s XP spectrum shows a single peak which is associated with adsorbed oxygen (Fig. 3, left panel). Therefore the higher energy component in Pd $3d_{5/2}$ level is ascribed to Pd bonding with adsorbed oxygen. From the spectral shapes and binding energies of the O 1s and Pd $3d_{5/2}$ components, this adsorbed oxygen is associated with the chemisorbed state.[2]

7. References

[1] R. Toyoshima, N. Hiramatsu, M. Yoshida, K. Amemiya, K. Mase, B. S. Mun and H. Kondoh, *J. Phys. Chem. C*, 2016, **120**, 416.

[2] R. Toyoshima, M. Yoshida, Y. Monya, Y. Kousa, K. Suzuki, H. Abe, B. S. Mun, K. Mase, K. Amemiya and H. Kondoh, *J. Phys. Chem. C*, 2012, **116**, 18691.

[3] Z.-H. Zeng, X.-F. Ma, W.-C. Ding and W.-X. Li, *Sci. China Chem.*, 2010, **53**, 402.

[4] A. Toyoshima, T. Kikuchi, H. Tanaka, K. Mase, K. Amemiya and K. Ozawa, *J. Phys.: Conf. Ser.*, 2013, **425**, 152019.

[5] S. Surnev, M. Sock, M. G. Ramsey, F. P. Netzer, M. Wiklund, M. Borg and J. N. Andersen, *Surf. Sci.*, 2000, **470**, 171.